REVIEW

Recent great impact by an Isotope Separator On-Line (ISOL) in nuclear and radiochemistry

Minoru Sakama

Department of Radiation Science and Technology, Institute of Biomedical Sciences, Tokushima University Graduate School, Tokushima, Japan

Abstract : On April 9 2015, the Letter article titled "Measurement of the first ionization potential of lawrencium, element 103" is now published at News and Views on Nature (2015) which has been performed by our remarkably Japanese colleagues of nuclear and radiochemistry at JAEA (Japan Atomic Energy Agency). In this review, the author will state that the isotope separator on-line (ISOL) our regularly used, one of mass separation techniques, with a thermal surface ionization makes possible for determining the ionization potential of lawrencium based on the fruitful fundations of developing the ISOL system until now and also ever studying searches for unknown nuclei and these nuclear decay properties around actinide region in the past 20 years. J. Med. Invest. 63 : 19-26, February, 2016

1 INTRODUCTION

On April 9 2015, the Letter Article (1) titled "Measurement of the first ionization potential of lawrencium, element 103" is now published on news and views on Nature (2015) which has been performed by our remarkably Japanese colleagues of nuclear and radiochemistry at JAEA (Japan Atomic Energy Agency). At the same time in this issue, this cover page entitled "EXTREME CHEMISTRY" has been adapted in praise of the present experimental challenge. The cover page shows the 3D-displayed periodic table of already known elements, in which each element symbol have been described with individually different bar sizes. In the cover page, their bar sizes represent energy levels of the first ionization potential (IP_1) for each of elements. In the principle of chemistry, a first ionization potential is one of most basic chemical properties in nature and its energy corresponds to the energy required to remove a single electron from an uncharged gaseous atom, whereby if all the first ionization potential energies characterized between the groups of elements have being found experimentally, their obtained trends play an important role not only to identify where the exact boundaries between elemental groups respectively should be located on the periodic table, but also to observe and understand Einstein's theory of relativity which would be possibly known for giving implications of various properties of atoms around heavier element region (2, 3) that have an atomic number (Z) greater than 100 such as lawrencium, element 103. In addition, we can obtain the present systematic experimental results related to IP on the periodic table around the heavy element region, and it will allow us to proceed exactly to effective improvements of theoretical calculations as estimating atomic and molecular orbital structures composed of material and also perhaps developing more functional materials toward future in the heavier element region.

In fact, the present great impact in chemistry has been exactly performed via none other than the JAEA Isotope Separator On-Line (JAEA-ISOL) (4-9) at the 20 MV Tandem accelerator facility in JAEA, Tokai, Ibaraki Japan, and then we have often used the instrument system for our related experiments of α-γ and γ-γ spectrometry and searching for new isotopes until now. At present, our experience in maintaining the mass separation techniques relative to the ISOL system has greatly contributed to foster them by ourselves to operate the ICP-DRC-QMS (Inductively Coupled Plasma Quadrupole Mass Spectrometry with a Direct Reaction Cell) (10) and those related devices such as an automatic chemical separation apparatus at Tokushima University (11, 12). Therefore, in this review article we will briefly review our several investigations including the present great impact which a gas-jet transport apparatus coupled to the ISOL system (5-9), in particular, this apparatus coupled with helium gas-jet aerosol transport system have ever performed around the actinides.

2 OVERVIEW OF THE JAEA ON-LINE ISOTOPE SEPARATOR (JAEA-ISOL) AT JAEA TANDEM ACCELERATOR

In nuclear sciences, that is mainly nuclear physics and nuclear and radiochemistry, an on-line isotope separator (13) with comparatively large size than commercial-based mass separation instruments such as ICPMS is good at nuclear identified and nuclear spectroscopic studies for unstable nuclei which are produced via nuclear reactions. In the 1960's, the development in the early stage, in which nuclei are produced and mass-separated through a continuous process, was started to be able to elucidate the new findings concerning these unstable and rare nuclei. This ISOL type of mass separation has been operated based on the basic mass separation principle similarly adapted for any other different type such as ICPMS (Inductively Coupled Plasma Mass Spectrometry) (14) and so on as follows ; at first, gas-aerosol mixture adsorbed reaction products (nebulized liquid mixture in the case of ICPMS) are transported to ion source site where these products are ionized with the mass-to-charge of m/z ($z = n \cdot e$ charged number of ion),

secondly ion separator site where these ionized nuclides are mass-separated and extracted by a few kV voltage, and finally ion detector site where the extracted and exact mass-separated ions of interest are detected as ion counting intensities.

So far, we have performed all the experiments relative to those nuclear sciences us-ing the JAEA on-line isotope separator (JAEA-ISOL) coupled with the helium gas-jet transport system (15, 16). A schematic view of the experimental setup (16) is shown in Figure 1. Induced ion beams from proton to heavy ion, e.g. boron-11 (^{11}B), were provided by the tandem accelerator located at the JAEA. The JAEA tandem accelerator is a type of electrostatic accelerators, which has two step accelerations of ion particles with one high voltage terminal. A faraday cup in the irradiation room was used to mea-sure the target beam current throughout all experiments and the signal was transmitted to the control rooms of both ISOL and the tandem accelerator. In the accelerator control room, the integrated charge was recorded continuously by a Multi-Channel Scaling (MCS) mode in a personal computer. The layout (16) of the beam line and irradiation room is shown in Figure 2. We have desirably announced that this irradiation room where we can regularly use various radioactive targets, for example plutonium and californium elements at irradiation experiments is the only unique facility in Japan. There are two beam lines named R-1 and R-2 at the irradiation room. The target recoil chamber was typically set at the end of the R-2 line. This beam line consists of two turbo-molecular pumps (TMPs) with the pumping speeds of 500 l/s and 270 l/s for dif-ferential pumping, in order to avoid contamination of the accelerator even if radioactive targets should have been broken. During the irradiation, the pressure inside the beam line, as monitored by a Penning vacuum gauge, was kept under 2×10^{-7} torr.
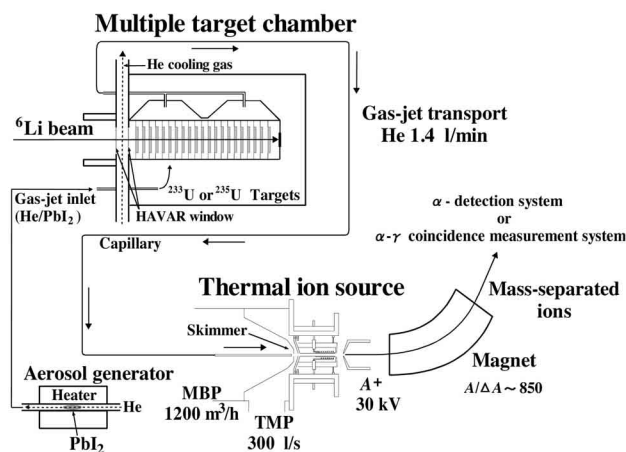

Figure 1 : Schematic view of the gas-jet coupled JAEA-ISOL (6, 16). The gas-jet trans-port system consists of the aerosol generator device, the multiple thin target chamber, and the vacuum system which consists of a mechanical booster pump (MBP) and a turbo-molecular pump (TMP) for the differential pumping.

3 DEVELOPMENT AND OPTIMIZATION OF THE GAS-JET TRANS-PORT SYSTEM COUPLED TO THE JAEA-ISOL

The JAEA-ISOL has been installed at the JAEA tandem accelerator in 1982 when the tandem accelerator also started for regular operation. In 1995, a primal gas-jet transport system coupled to a thermal ion source was installed in the ISOL system (5). At this
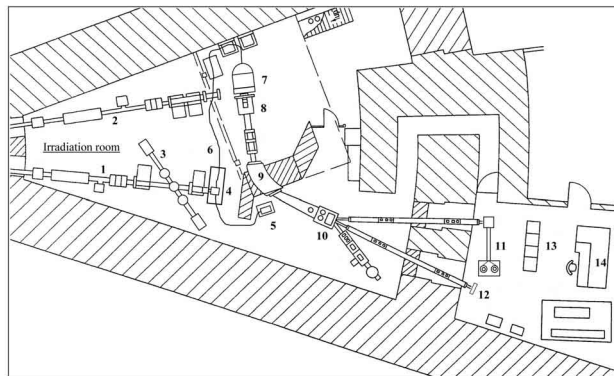

Figure 2 : Layout of the irradiation room at the JAEA tandem accelerator (6) : (1) R-2 line, (2) R-1 line, (3) TOF chamber, (4) target chamber and glove box, (5) aerosol gen-erator, (6) capillary, (7) ion source, (8) extraction chamber, (9) magnet, (10) collection chamber, (11) tape transport system or ion-implanted detection system, (12) rotating-wheel α-detection system or α-γ(γ)-rays coincidence measurement system, (13) data acquisition system, and (14) control console for ISOL.

time, it was utilized to search for unknown neutron-rich rare-earth isotopes produced in the proton-induced fission of ^{238}U. In the reference (15), Ichikawa *et al.* had reported that the NaCl/Ar gas-jet transport system coupled with the JAEA-ISOL using a NaCl aerosol cluster had separation efficiencies of a few percent for the isotopes of $_{55}$Cs to $_{63}$Eu except for the very short-lived nuclei. Thereafter, increase of these separation efficiencies of this combined system was accomplished and it enabled to identify new neutron-rich ^{159}Pm, ^{162}Sm, ^{166}Gd, and ^{166}Tb.

During the course of the investigation on decay properties of new neutron-deficient actinides, a multiple thin target chamber system coupled to the JAEA-ISOL using a PbI$_2$ aerosol cluster in a helium gas-jet instead of the NaCl aerosol cluster in an argon gas-jet has been developed to identify these still unknown nuclides of intrest around the actinide region. Regularly used operation parameters of the on-line isotope sepa-rator are summarized in Table 1, and then schematic drawing of the configuration of ion optics (16) for ISOL is also shown in Figure 3. This instrument, DANFYSIK$^{\copyright}$ belongs to the type of ISOLDE (4) and its fundamental concept of ion separation for nuclides is fairly similar to those systems of GSI (GSI-ISOL) (17) and CERN (CERN-ISOLDE) (18). Comparing the previous ISOL system (16) with the present one (19), as shown in both the Figures 1 and 4, with explaining an ionization framework and a separation technique on those systems, and thus the set up consists of a multiple target chamber (for Am, Np, Cm, and Bk around the neutron-deficient still unknown nuclide region) or a target-recoil chamber (for Fm, Md, No, and Lr) coupled to an aero-sol gas-jet trasport device, a surface ion-source, a mass separator, and a detection system for those nuclear decays.

For the neutron deficient $_{95}$Am experiment (16, 20-22), multiple thin targets of ^{233}U or ^{235}U (thickness about 100 to 400 μg cm^{-2}) in the multiple target cham-ber, as shown in Figure 1, were irradiated with 45.5-MeV, 51.0-MeV, and 63.0-MeV ^{6}Li^{3+} ion beams delivered from the tandem accelerator at the JAEA and then for the Lr ex-periment (1, 19) a ^{249}Cf target (thickness 260 μg cm^{-2}) in the target-recoil chamber (in Figure 4) was irradiated with a 67.9-MeV ^{11}B^{4+} beam also delivered from the same accelerator. Nuclear reaction products, recoiling from the target, attached onto PbI$_2$ or CdI$_2$ particles produced by sublimation of their compounds, were trans-ported to the ionization cavity of the ion-source installed in the JAEA-ISOL (5, 8).

At early stage for the development of gas-jet transport device coupled to the JAEA-ISOL (15), the multiple target chamber and

Table 1 : Parameters of the JAEA on-line isotope separator (JAEA-ISOL) (6).

1) Product type	DANFYSIK© 9000-T (made in Sweden)
2) Ion source	Gas-jet coupled to a thermal ion source
3) Acceleration	Extractor (≦ 100 kV), Y-deflector
	Einzellense E1 (d = 120 mm), E2 and E3 (d = 70 mm)
	Quadrupole doublet (d = 100 mm)
4) Magnet	Double-focusing 55° magnet
	Orbit radius = 1500 mm
	Magnet field = 500 Gauss (maximum)
	Deflection angle = 55°
	Inclination (entrance) = 0°, (exit) = 35.5°, Gap = 55 mm
5) Collection	Faraday cup, Collector plate, Beam profile monitor,
	25° deflector
6) Beam transmission line (BTL)	Left[a] (+25°), Center[b] (0°), Right[c] (-25°)
7) Beam emittance	2 mm ϕ
8) Transmission	about 90% to focal plane chamber
9) Energy spread	< 10 eV
10) Mass dispersion	$\frac{1500}{M}$ mm ; M is a central mass number
11) Mass range	1 up to 270 amu for 100 keV ions (1+)
12) Mass resolving power	1500 (maximum)
13) Entrance-slit width at a focal plane	7 mm
14) Cross-contamination	< 0.001% for neighboring masses
15) Mass Accuracy/Positioning	0.014 amu/0.1 mm

[a]For a tape collection system and an ion-implanted detection system
[b]For a rotating-wheel α-detection system and α-γ (γ)-rays coincidence measurement system
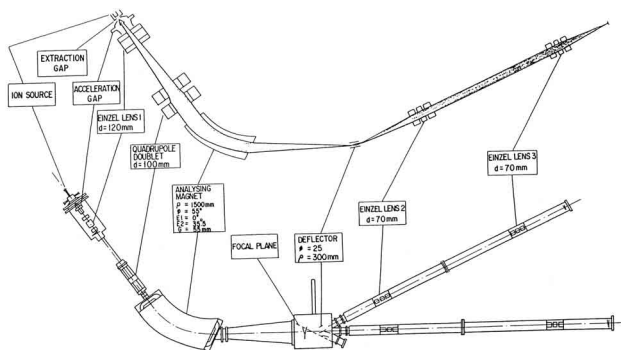[c]for a laser spectroscopy (other purpose)

Figure 3 : Configuration of the ion optics of the JAEA on-line isotope separator (6). Horizontal beam envelopes are magnified in the top of this figure.
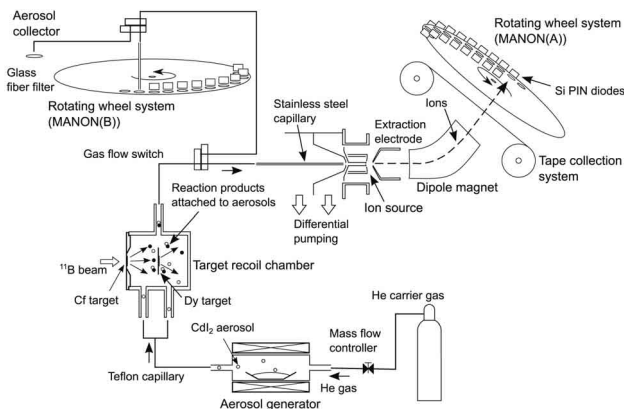

Figure 4 : Referred to the article (19) of T.K. Sato, *et al.* Schematic drawing of the helium/CdI₂ gas-jet transport apparatus coupled to the JAEA-ISOL for the Lr experi-ments.

the skimmer-ion source part, as shown in Figure 1, are connected with an 8 m long Teflon® capillary tube of ϕ 1.4 mm. A helium gas loaded with the PbI₂ aerosol cluster in the capillary was used as the carrier gas for the transport of the nuclear reaction products. The reaction products recoiling out of a thin target were slowed to the thermal energy in the helium gas at a pressure near the atmospheric one, and the thermalized atoms were transported together with the helium gas to the skimmer-ion source by differential pumping through the 8 m long Teflon® capillary. Two-skimmer chambers were skimming off the helium gas. The orifices of the first and second skimmers were ϕ 2 mm and ϕ 6 mm in diameter, respectively. The pumping device had been composed of two turbo-molecular pumps (TMP ; 1800 l/s and 300 l/s for the 1st and 2nd skimmer chamber, respectively). However, the improved setup has been equipped with a 1200 m³/h roots pump (BOC EDWARDS© EH-1200) and the 300 l/s pump of the two TMPs to increase pumping capacity, which allows a significant skimming-off of the helium flow in the first skimmer chamber. It brought that the distance between the stainless capillary end and the first skimmer could be reduced from 5 mm to 4 mm, and this seems to contribute to suppress a transmission loss of the aerosol stream in the first skimmer. This transmission loss may be caused by the half-angle of the divergence of the aerosol stream. At a helium gas flow rate of 1.4 l/min during a typical operation of its system, the gas pressure attained 10 Pa in the second skimmer compartment and 1.2×10⁻⁵ Pa in the extraction chamber. To prevent glow discharges and sparks between the components of the ion source and the two pumping devices, the differential pumping system was held at the same potential of +30 kV as that of the ion source chamber.

This type of ion source whose ionizer is heated to high temperature can give high ionization efficiencies for lanthanides and elements of alkaline metals. Kirchner (13) has reported surface ionization efficiencies for various ionizing surfaces and Pilzer (23) has also discussed ionization of the lanthanides in a hot cavity. For a thermally equilibrated system at high temperature T, Nernst's heat theorem (24) permits us to calculate the equilibrium constant.

For example, if A is the atom to be ionized, in the reaction of $A \rightleftharpoons A^+ + e^-$, the equilibrium constant has been calculated by Eggert with the values of the absolute entropies based on molecular partition functions of the atom(A)-, ion(A$^+$)-, and electron(e$^-$)-gas.

$$\frac{n_e n_i}{n_0} = \left(\frac{2\sigma_i}{\sigma_0}\right) \times \left(\frac{2\pi mkT}{h^2}\right)^{3/2} \exp\left(-\frac{IP_i}{kT}\right) \tag{1}$$

This function is well-known as Eggert-Saha-equation (25, 26) : n_0, n_i, and n_e denoting the respective densities of the atoms A, the ions A$^+$ and the electron e$^-$, IP$_i$ the ioniza-tion potential of the atoms, σ_i and σ_0 the energies and statistical weights of the ionic or atomic ground state, m the electron mass, k Boltzmann constant, h Plank constant, and T temperature of the surface. Here, the electron density n_e may be expressed by the following equation of the Richardson's law :

$$n_e = 2\left(\frac{2\pi mkT}{h^2}\right)^{3/2} \exp\left(-\frac{\phi}{kT}\right) \tag{2}$$

ϕ being the work function of the electron emitter. Inserting eq. (2) into eq. (1) gives

$$\alpha = \frac{n_i}{n_0} = \left(\frac{\sigma_i}{\sigma_0}\right) \exp\left[\frac{(\phi - IP_i)}{kT}\right] \tag{3}$$

$$\beta = \frac{n_i}{(n_i + n_0)} = \frac{\alpha}{(1+\alpha)} \tag{4}$$

where β corresponds to the surface ionization efficiency I_{eff}, that is experimental values, they will be led by the coefficient term of σ_i/σ_0, as shown in the equation (3), obtained directly using the ISOL system with an ion-source type based on thermal surface ionization phenomena of atoms. Those equations are based on the Langmuir-equation for the ionization degree of negative surface ionization. From the equation 4, surface ionization efficiencies for the material Re (rhenium) and W (tungsten) were calculated. Figure 5 provides plots of their surface ionization efficiencies of β. It is revealed that the ionization efficiency as a general behavior strongly depends on both temperature of the surface and ionization potential in the region of IP$_i$ > ϕ. It is confirmed that the ionization

efficiency of Re at temperature (2450 K) is about 20 times higher than that of W, because the work function ϕ of the electron emitter of Re is 5.1 eV higher than that of W (ϕ = 4.5 eV). Therefore, the inner wall of the ionizer was covered with a thin Re foil, although W was utilized for making up the ionizer because of its good plasticity.

The ionizer was heated by thermal radiation and by the electrons from the tung-sten filament. With the filament heated by an input power of about 450 W, electrons emitted from the filament were accelerated toward the ionizer which was biased at 450 V against the filament's potential. When the electron current for bombard-ment is increased to 1 A, it is known from the previous observation data (5) that the temperature near the outlet aperture of the anode reaches as high as 2450 K. Table 1 summarizes the regularly used parameters (6) for operation and performance of the helium gas-jet coupled with the JAEA-ISOL. In particular, the ionization efficiency in the surface ionization and the mass resolution in the focused mass region are important factors and give large influence on identification of new isotopes and investigations for still unknown nuclides on their nuclear properties. Theoretical ionization efficiencies, as deduced from Figure 5, are summarized for the elements Bk, Am, and Cm in Table 2 (6). It has indicated that those elements have possessed next to the same as an ionization efficiency in comparison with other lanthanides (Sm, Dy, and Ho). It is, therefore, sug-gested that the JAEA-ISOL system should make possible ionizations of Am, Cm and Bk elements. Using the developed at early stage of the our composite analyzing system consists of the helium/PbI$_2$ gas-jet transport apparatus and the thermal ion-source in the JAEA-ISOL, we have searched for new isotopes and study Electron Capture (EC) and Alpha decay properties (6) of these neutron-deficient actinides.

Table 2 : Ionization potentials and theoretical ionization efficiencies of focused actinides and other lanthanides (6).

Element	IP$_i$^{a}/eV	Ionization efficiency/%
Am	5.99	1.5
Cm	6.02	1.3
Bk	6.23	0.5
Sm	5.64	7.2
Dy	5.94	1.8
Ho	6.02	1.3

^{a}Refer to *Handbook of Chemistry and Physics, 75th* edition, D.R. Lide, editor, CRC Press, (1995).
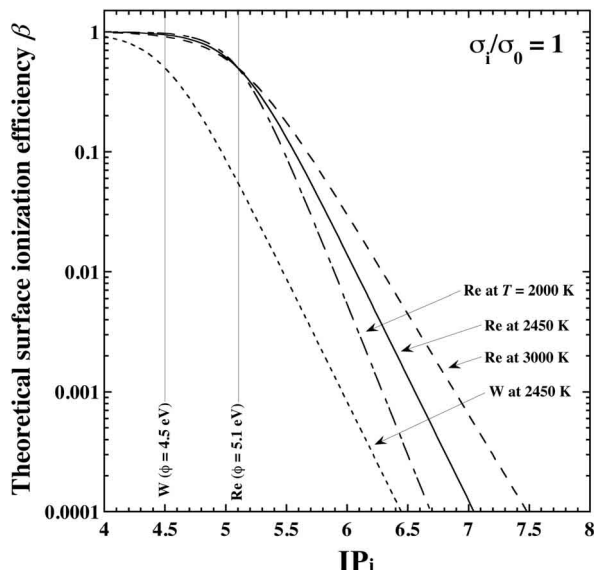
Figure 5 : Theoretical surface ionization efficiency (6) of an arbitrary element Z (e.g., $_{82}$Pb for PbI$_2$, $_{19}$K for KCl, $_{95}$Am, and $_{103}$Lr) versus its ionization potential IP$_i$ for the ionizer material rhenium (Re) and tungsten (W). Curves are calculated for σ_i/σ_0 = 1, it can be used for any ratio of statistical weights, if IP$_i$ is replaced by the effective value IP$_i'$ = IP$_i$ − kT ln (σ_i/σ_0).

For the $_{103}$Lr experiments of determining the first ionization potential of IP$_1$, the present great impact in nuclear and radiochemistry has been created by steady progress on the development of the gas-jet coupled to the JAEA-ISOL. The developed ion-source at the early stage that already provided good ionization efficiency for lanthanides as mentioned above had been implemented with further progress ; the cylindrical ionizer made of a (Ta) tantalum crucible was newly surrounded by two (W) tungsten filaments. Additionally the two heat shields were rearranged to effectively heat the ionizer (19). The newly set up filament (19) is shown as Filament 2 in Figures 6(a) and 6(b). The ionizer was heated by both thermal radiation from the filaments and the electron bombardment. For thermal heating, regularly used an electrical power was set about 200 W up for each filament. Having slightly controlling the input power for Filament 1, providing differences in the power of the electron bombardment from Filament 1 and it made possible setting up the temperature of the ionizer properly. The voltage for the electron bombardment was continually kept
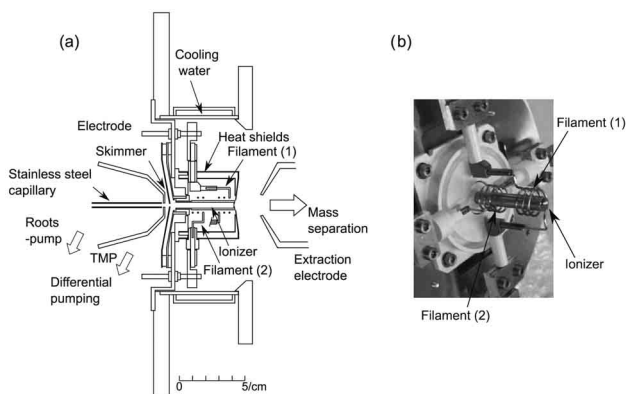
Figure 6 : Referred to the article (19) of T.K. Sato, *et al.* (a) Schematic drawing of the surface ionization type ion-source with the skimmer system and the extraction electrode of the ISOL. (b) Photograph view of the new arrangement of the ionizer. An additional filament is installed as indicated Filament 2.

Figure 7 : Expected profiles (6) for extraction ion beams of Mass = 236, 237, and 238. An entrance-slit width of 7 mm at focal plane is indicated by vertical bold lines around the center of mass = 237, which approximately corresponds to the mass dispersion 7 mm in the ISOL system.

constant at 450 V. The elec-tric power for heating each filament and for the electron bombardment was controlled independently. The input power of the electron bombardment from the Filament 2 was kept constant at 99 W (450 V × 0.22 A). When the electric power of the elec-tron bombardment from Filament 1 reached 450 W (450 V × 1.0 A), the temperature next to the outlet of the ionizer was approximately 2600 K measured with an optical pyrometer. CdI_2 was used as an aerosol material for transportation because (a) it is heavy enough to give a good skimmer efficiency, (b) the elements are tolerable in the hot ionizer, and (c) it has a sufficiently low boiling point of 713°C to rapidly evaporate all aerosol material. The CdI_2 aerosols (19) carrying nuclear reaction products passed through the skimmers, and were immediately vaporized at the surface of the ionizer. The reaction products were desorbed and ionized via the surface ionization process at the surface, and were extracted by the extraction electrode and accelerated toward the analyzing dipole magnet as shown in Figure 4.

Then, regarding the mass resolution performance of the JAEA-ISOL, the entrance-slit width at the focal plane was set to be 7 mm for fully exploiting its mass resolu-tion power and then for suppressing the cross-contamination from neighboring masses. Characteristic mass dispersion D for the JAEA-ISOL system can be expressed as $D = 1500/M$ (mm) where M is a focused central mass number. The mass dispersion D was chosen as 7 mm which corresponded to the entrance-slit width. The mass res-olution of $M/\Delta M$ was measured by observing the profiles of analyzed beams for lead stable isotopes, ^{206}Pb, ^{207}Pb and ^{208}Pb which were contained in the PbI_2 aerosol clus-ters. The value was experimentally measured by a beam profile monitor in the console frame of JAEA-ISOL. The mass resolution could be evaluated to be about 800 at the fo-cal plane of the magnet. In addition, in order to understand this performance using the entrance-slit width of 7 mm in the JAEA-ISOL, the cross-contamination was estimated for i.e. $A = 237$ from the both neighboring masses 236 and 238. In general, the beam profile at the focal plane in the switchyard may be assumed to be the Lorentzian distri-bution. Simulating the fictitious beam profiles for A = 236, 237 and 238, respectively, based on the Lorentzian distri-bution, their beam profiles (6) become as plotted in Figure 7 if each of the beam intensities is equal. In Figure 7, the entrance-slit (shown by the vertical bold lines) of 7 mm width, that also corre-sponds to the mass dispersion, has been set around the center of A = 237. It can be deduced that the cross-contamination originated from the tails of the neighboring mass 236 and 238 beams should be as little as 0.00083%. Therefore, this mass resolution power
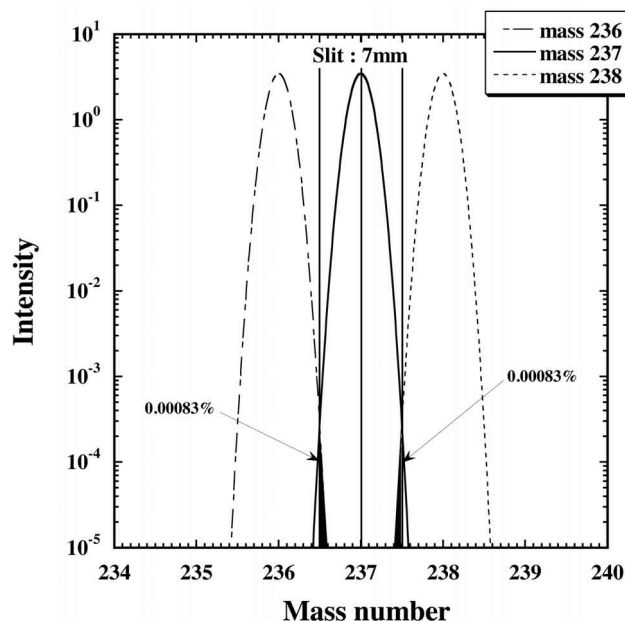
should unambiguously benefit the mass identification of unknown americium isotopes.

4 RECENT GREAT IMPACT AND STUDIES OF NUCLEAR AND ATOMIC PROPERTIES ON CHEMISTRY AND PHYSICS BY THE GAS-JET TRASPORT SYSTEM COUPLED TO THE JAEA-ISOL

There still remain a lot of unknown nuclides to be discovered in the region of neutron-deficient actinides which predominantly decay through the electron capture (EC) (27-30). Decay proper-ties of these nuclides lead to considerable advances in the un-derstanding of proton excess heavy nuclei such as complicated hexa-decapole deformation (31, 32), and more characteristic fission barrier heights of neutron-deficient nuclei far from the nuclear stability region such as EC-delayed fission.

As for searching the unknown isotopes and investigating the EC- and Alpha-decay properties in the neutron-deficient americium element Am and around the region of the daughter nuclides using the JAEA-ISOL, Table 3 summarizes the α-decay prop-erties of the neutron-deficient Am and Np isotopes observed using the JAEA-ISOL in also including their estimated production cross section experimentally. The new ex-perimental α-decay properties are summarized principally regarding half-lives $T_{1/2}$, α-particle ener-gies E_α and α branching ratios I_α. A new isotope ^{233}Am has been iden-tified for the first time during the course of this study (20). For ^{235}Am, the α-decay process has been observed for the first time and the α-branching has been derived from the ratio between the ob-served α and Pu K x-ray intensities. Additionally, this study could attain more precise data on the nuclear decay properties of ^{234}Am and ^{236}Am (16, 33, 34). By dealing with the new measured α-and EC-decay data, this thesis have elucidated the systematic trend of the α-transition probability and mass excess values in the region of neutron-deficient actinides. The discussion has resulted in much more precious and characteristic nuclear decay properties in terms

Table 3 : Alpha-decay properties of the neutron-deficient Am and Np isotopes observed using the JAEA-ISOL (16). The production cross sections are evaluated using the overall efficiency of $0.3\pm0.1\%$ for americium atoms based on the present JAEA-ISOL performance.

Nuclide	Reaction	Experimental production cross sections and decay properties by the JAEA-ISOL			
		σ_{exp} (μb)	$T_{1/2}$ (min)	E_α (keV)	I_α
^{236}Am^{g+m}	^{235}U(^{6}Li,5n)	125 ± 46	3.6 ± 0.1	6150	$(4.0\pm0.1)\times10^{-5}$
^{235}Am	^{233}U(^{6}Li,4n)	31 ± 12	10.3 ± 0.6	6457 ± 14	$(4.0\pm0.5)\times10^{-3}$
	^{235}U(^{6}Li,6n)	5 ± 2			
^{234}Am	^{233}U(^{6}Li,5n)	9 ± 5	3.5 ± 1.3	not observed	$<4\times10^{-4}$
^{233}Am	^{233}U(^{6}Li,6n)	<0.9	3.2 ± 0.8	6780 ± 17	$>3\times10^{-2}$
^{229}Np	it is α-decay daughter of ^{233}Am		4.0 ± 0.4	6893 ± 23	0.68 ± 0.11

of nuclear sciences. The α-particle energies (16) of ^{233}Am and ^{235}Am were determined to be 6780 ± 17 keV and 6457 ± 14 keV, and their half-lives were measured to be 3.2 ± 0.8 min and 10.3 ± 0.6 min, respectively. The α branching ratios I_α of ^{235}Am and of ^{229}Np, the α-decay daughter of ^{233}Am, were determined to be $(4.0\pm0.5)\times 10^{-3}$ and 0.68 ± 0.11, respec-tively, and the lower limit of α branching ratio for ^{233}Am was deduced to be 3×10^{-2}. Using a well-known systematic formula relating α-particle partial half-life $T^\alpha_{1/2}$ and α-transition energy E^*_α, we have evaluated the hindrance factors for odd-A Am and Np and for even-A Am. It was found that those observed α transitions of ^{233}Am, ^{235}Am, ^{236}Am, and ^{229}Np had hindrance factors close to unity, and thus, they could be regarded as the favored transitions (16). In addition, we have obtained the experimental data as Q_α (expt) value of ^{233,235,236}Am derived from their measured α-particle energies.

On the production cross section data of americium isotopes, it has been found that the production cross sections were evaluated using the overall efficiency (16) of $0.3\pm0.1\%$ for americium atoms using the JAEA-ISOL system. Figure 8 shows ex-citation function curves (6) of the ^{233}U(^{6}Li,xn)$^{239-x}$Am and ^{235}U(^{6}Li,xn)$^{241-x}$Am which were calculated by the statistical model calculation ALICE code (35). Data points of the observed production cross sections and the previous one as a function of incident ^{6}Li beam energy are plotted in the figure. For the ^{233}U(^{6}Li,4n)^{235}Am reaction, the ob-served production cross section is in a large discrepancy with the predicted one by a factor of about 2.2 as shown in Fig. 8. However, in all the other Am isotopes, the data points of the observed production cross sections fall on the excitation function curves predicted by the ALICE code (35). It has indicated that the ALICE code can be used for estimating production cross sections of still unknown Am nuclides produced via the bombardment of ^{233}U and ^{235}U with ^{6}Li from resulting in approximately agreement between the experimental data and the estimated ones.

For the latest and great impact (1, 19) of experimentally determining the first ioniza-tion potential (IP$_1$) for lawrencium element $_{103}$Lr by the helium/CdI$_2$ gas-jet apparatus coupled to the JAEA-ISOL system, this review paper has outlined the following proce-dure below. At first, there is a need to analyze the I_{eff} values of short-lived lanthanide and alkali isotopes which were produced via nuclear reactions of ^{11}B beams with target materials, and then to take as much as possible a large number of such various element's I_{eff} values. And all the obtained data points will allow us to deduce the ion-ization efficiency I_{eff} of the various short-lived isotopes more precisely as a function of the effective IP$_1$ (IP$^*_1$) at 2700 K in the thermal surface ion-source. Here is, in order to calculate those I_{eff} values, the number of atoms transported to the ion-source was de-termined via a direct-catch measurement, and the number in-cludes what the ionization efficiency should be equal to 100% before vaporizing and ionizing each of the atoms for those short-lives isotops into a cavity of thermal surface ion-source at the ISOL system. The relationship between IP$^*_1$ and I_{eff}, as shown in Figure 9, provided such a fitting curve expressed as the function in equations
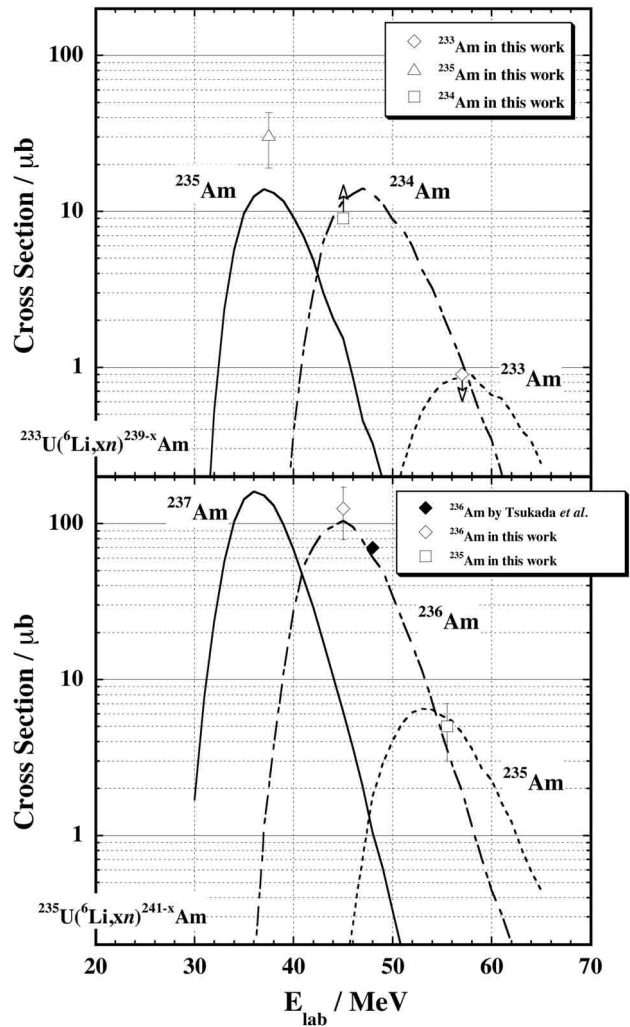

Figure 8 : Excitation functions (6) for the ^{233}U(^{6}Li,xn) (x=4, 5, and 6 neutron channels) in the upper figure and ^{235}U(^{6}Li,xn) (x=4, 5, and 6 neutron channels) reactions in the lower figure. The solid and broken lines illustrate the predicted excitation functions by the ALICE code (35). E$_{lab}$ means the beam energy in the laboratory system. Insert of the previous cross section data of ^{236}Am is referred to the article (9) of K. Tsukada, *et al.*

(3) and (4). As subjected to the most appropriate fitting curve function with reproducing those data points at each short-lived isotope, those results made experimentally possible to determine the free coefficient pa-rameter of σ_i/σ_0 value which is associated with the energies and statistical weights of the ionic or atomic ground state
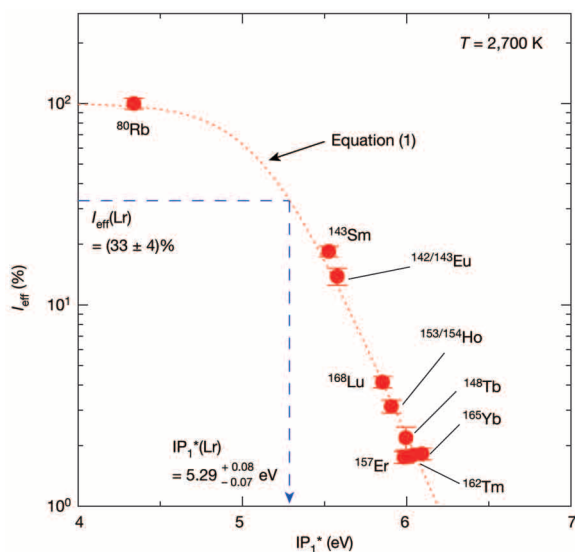
Figure 9 : Referred to the article (1) of T.K. Sato, *et al.* The ionization efficiency I_{eff} of various short-lived isotopes as a function of the effective IP$_1$ (IP$_1^*$) at 2700 K. The short-dashed curve is obtained by fitting the experimental data using equation (4), which describes a relationship between I_{eff} and IP$_1^*$ in the present system. The position of the measured I_{eff} value of Lr, that is (33 ± 4)%, is also shown. From the fitted equation (4) with $\sigma_i/\sigma_0=43\pm3$, IP$_1^*$ of Lr is calculated to be $5.29^{+0.08}_{-0.07}$ eV. This corresponds to an IP$_1$ value of $4.95^{+0.10}_{-0.08}$ eV at 2700 K. Error bars, ± 1s.d.

at $T=2700$ K and 2800 K, respectively. Energies and statistical weights of low-lying states in the ion and the atom of each element were cited from the National Institute of Standards and Technology (NIST) atomic database. The I_{eff} values determined for all isotopes were best fitted with equations (3) and (4) using σ_i/σ_0 values of $43\pm$ 3 and 50 ± 3 at $T=2700$ K and 2800 K. The Lr IP$_1^*$ values of $5.29^{+0.08}_{-0.07}$ eV and $5.33^{+0.11}_{-0.10}$ were determined from equation (4) at T = 2700 K and 2800 K. The result at 2700 K is shown in Figure 9. Statical errors on the IP$_1^*$ value mainly due to three sources of uncertainty : surface temperatures, I_{eff} (which is caused to counting statistics) and fitting procedures. The Lr IP$_1$ can be calculated from IP$_1^*$ using the following equation (5) with Q_i and Q_0 (26),

$$\text{IP}_1^* = \text{IP}_1 - kT \ln\frac{Q_i}{Q_0}, \tag{5}$$

where Q_i and Q_0 are the partition functions at each temperature for the ion and the atom which can be calculated using excitation energies and statical weights of their ground and excited states based on the thermodynamics principle between the ionized and the atomic states. The energies and statistical weights for calculating Q_i and Q_0 were given as the estimated values based on relativistic Fock space coupled cluster (FSCC) calculations (36). The average absolute error for the 20 lowest excitation energies of lutetium, Lu (where comparison with experiment is possible) was 0.05 eV using the same approach. Therefore, it has been expected that the predicted transition energies of Lr would belong with such a similar accuracy, that is the evaluated values of $kT \ln Q_i/Q_0$ for Lr at $T=2700$ K and 2800 K provide $-0.34^{+0.06}_{-0.04}$ and $-0.36^{+0.06}_{-0.04}$, respectively. The error includes an uncertainty in the calculated excitation excitation energies indicated in 0.087 eV for each state in the temperature. As a result, using the the IP$_1^*$ value, the IP$_1$ values of $4.95^{+0.10}_{-0.08}$ eV and $4.97^{+0.13}_{-0.11}$ eV were obtained at $T=2700$ K and 2800 K, respectively. From these results, the first ionization potential IP$_1$ value of Lr has been determined to be $4.96^{+0.08}_{-0.07}$ eV experimentally (1).

The great impact includes that the gas-jet transport system coupled to the JAEA on-line isotope separator (JAEA-ISOL), which

has been newly improved and developed with more higher perfomance at present, allows us to elucidate that the IP$_1$ of Lr is distinctly lower than that of Lu. Lawrencium has the lowest IP$_1$ value of all lanthanides and actinides ; this quantitatively reflects and confirms the theoretically predicted sit-uation of closed $5f^{14}$ and $7s$ shells with an additional weakly-bound electron in the valence orbital which is similar to the situation for lanthanide series of closed $4f^{14}$ and $6s$ ones of Lu.

5 CONCLUSION AND PERSPECTIVE

In this review, the author has stated how the JAEA on-line isotope separator, which is coupled with the helium gas-jet transport apparatus, has been developed with overcom-ing some problems, and how this quite unique system has ever produced good results on nuclear science in the past 20 years. Based on the fruitful foundations of such a long term of developing the JAEA-ISOL, the system provided the recent great impact in nuclear and radiochemistry that the first ionization potential IP$_1$ value of Lr has been for the first time determined to be $4.96^{+0.08}_{-0.07}$ eV experimentally. The author has emphasized that the surface ionization method on the isotope separator on-line, successfully applied here to determine the ionization potential of Lr, can provide experimental data around other heavier actinides, e.g. fermium $_{100}$Fm, mendelevium $_{101}$Md, and no-belium $_{102}$No, and also can estimate quantum chemical calculations of the heaviest elements. At present, the author and research colleagues have already begun to imple-ment the on-line experiments of measurements for the ionization potentials of Fm, Md, and No using the JAEA-ISOL. Finally, it opens up new perspectives on determining ba-sic atomic properties of the superheavy elements and aslo the author believes that the on-line isotope separator (ISOL) is an indispensable tool for fulfilling the perspectives in future.

CONFLICT OF INTEREST STATEMENT

The Author declares no conflict of interest associated with this manuscript.

ACKNOWLEDGEMENT

REFERENCES

1. Sato TK, Asai M, Borschevsky A, Stora T, Sato N, Kanaya Y, Tsukada K, Düllmann ChE, Eberhardt K, Eliav E, Ichikawa S, Kaldor U, Kratz JV, Miyashita S, Nagame Y, Ooe K, Osa A, Renisch D, Runke J, Shädel M, Thörle-Pospiech P, Toyoshima A, Trautmann N : Measure-ment of the first ionization potential of lawrencium, element 103. Nature 520 : 209-211, 2015

2. Shädel M : Chemistry of Superheavy Elements, Angew. Chem. Int. Ed. 44, Wiley-VCH Verlag GmbH & Co. KGaA, Weinheim : 368-401, 2006

3. Nagame Y, Asai M, Haba H, Tsukada K, Goto S, Sakama M, Nishinaka I, Toyoshima A, Akiyama K, Ichikawa S : Status and prospects of heavy element nuclear chemistry research at JAERI. J Nucl and Radiochem Sci 3(1) : 129-132, 2002

4. Nielsen BR : Improved resolving power of an isolde type isotope separator. Nucl Instrum Methods 186 : 457-461, 1981

5. Ichikawa S, Asai M, Tsukada K, Osa A, Ikuta T, Shinohara N, Iimura H, Nagame Y, Hatsukawa Y, Nishinaka I, Kawade K, Shibata M, Kojima Y : Mass separation of neutron-rich isotopes using a gas-jet coupled thermal ion source. Nucl Instr and Meth A 374 : 330-334, 1996

6. Sakama M : *Ph. D. thesis,* Alpha-decay properties of neutron deficient ameri-cium isotopes, TMU-1123, Tokyo Metropolitan University, 2004

7. Ichikawa S : *Ph. D. thesis,* Nagoya University 1996.

8. Ichikawa S, Tsukada K, Asai M, Osa A, Oura Y, Iimura H, Kojima Y, Hirose T, Nishinaka I, Hatsukawa Y, Nagame Y, Kawade K, Ohyama T, Sueki K : Search for unknown isotopes using the JAERI-ISOL. Nucl Instr and Meth B 126 : 205-208, 1997

9. Tsukada K, Ichikawa S, Hatsukawa Y, Nishinaka I, Hata K, Nagame Y, Oura Y, Ohyama T, Sueki K, Nakahara H, Asai M, Kojima Y, Hirose T, Yamamoto H, Kawade K : Half-life of the electron capture decaying isotope ^{236}Am. Phys Rev C 57 : 2057, 1998

10. Takahashi J, Yamada N : Development of collision/reaction for reduction of spectral interference in ICP mass spectrometry. : BUNSEKI KAGAKU 53(11) : 1257-1277, 2004

11. Sakama M, Saze T, Kitade T, Shikino O : Development of elemental and isotopic analysis of uranium and thorium in material using an automatic SPE injection equipment coupled to ICP-DRC-MS. : International Journal of Modern Physics B 25(31) : 4175-4179, 2011

12. Sakama M, Nagano Y, Saze T, Higaki S, Kitade T, Izawa N, Shikino O, Nakayama S : Application of ICP-DRC-MS to Screening Test of Strontium and Plutonium in Environmental Samples at Fukushima. : Applied Radiation and Isotopes 81 : 201-207, 2013

13. Kirchner R : Progress in ion source development for on-line separators. Nucl Instrum Methods 186 : 275-293, 1981

14. Houk RS, Fassel VA, Flesch GD, Svec HJ, Gray AL, Taylor CE : Inductively coupled argon plasmas as ion sources for mass spectrometric deter-mination of trace elements. Anal Chem 52 : 2283-2289, 1980

15. Ichikawa S, Tsukada K, Asai M, Haba H, Sakama M, Kojima Y, Shibata M, Nagame Y, Oura Y, Kawade K : Performance of the multiple target He/PbI$_2$ aerosol jet system for mass separation of neutron-deficient actinide isotopes. Nucl Instr and Meth B 187 : 548-554, 2002

16. Sakama M, Asai M, Tsukada K, Ichikawa S, Nishinaka I, Nagame Y, Haba H, Goto S, Shibata M, Kawade K, Kojima Y, Oura Y, Ebihara M, Nakahara H : α-decays of neutron-deficient americium isotopes. Phys Rev C 69 : 041308, 2004

17. Kirchner R, Burkard KH, Huller W, Klepper O : The ion sources for the GSI on-line separator. Nucl Instrum Methods 186 : 295-305, 1981

18. Sundell S, Ravn H, ISOLDE collaboration : Ion source with combined cathode and transfer line heating. Nucl Instrum Methods B 170(1-4) : 160-164, 1992

19. Sato TK, Sato N, Asai M, Tsukada K, Toyoshima A, Ooe K, Miyashita S, Schädel M, Kanaya Y, Nagame Y, OsaA, Ichikawa S, Stora T, Kratz JV : First successful ionization of Lr (Z=103) by a surface-ionization technique. Rev Sci Instrum 84 : 023304, 2013

20. Sakama M, Tsukada K, Asai M, Ichikawa S, Haba H, Goto S, Oura Y, Nishinaka I, Nagame Y, Shibata M, Kojima Y, Kawade K, Ebihara M, Nakahara H : New isotope ^{233}Am. Eur Phys J A 9 : 303-305, 2000

21. Asai M, Tsukada K, Ichikawa S, Sakama M, Haba H, Nishinaka I, Nagame Y, Goto S, Kojima Y, Oura Y, Shibata M : α decay of ^{238}Cm and the new isotope ^{237}Cm. Phys Rev C 73 : 067301, 2006

22. Asai M, Tsukada K, Ichikawa S, Sakama M, Haba H, Nagame Y, Akiyama K, Toyoshima A, Kaneko T, Oura Y, Kojima Y, Shibata M : Identification of the new isotope ^{241}Bk. Eur Phys J A 16 : 17-19, 2003

23. Pilzer EH, Engler G : A new ion source for fission-yield measurements of rare-earth isotopes. Nucl. Instrum. Methods B 26 : 218-222. 1987

24. Nernst W : *Die theor. und exp. Grundlagen des neuen Wärmesatzes* (Knapp-Verlag, Halle, Saale, 1918), chap. XI.

25. Kirchner R : On the thermoionization in hot cavities. Nucl Instrum Methods A 292 : 203-208, 1990

26. Zandberg ÉY, Ionov NI : Surface ionization. Sov Phys Usp 2 : 255-281. 1959

27. Shinohara N, Novikov YN, Münzenberg G, Wollnik H, Hatsukawa Y, Asai M, Tsukada K, Osa A, Oshima M, Haba H, Ichikawa S, Nagame Y, Popov AV, Seliverstov DM : Search for "missing" α-emitters for the mass mapping of superheavy elements. JAERI-Review 029 : 45-46, 2002

28. Hall HL : Ph. D. thesis, Delayed-fission properties of neutron-deficient ameri-cium nuclei, LBL-27878, Lawrence Berkeley Laboratory, 1980

29. Higgins GH : Ph. D. thesis, An investigation of the isotopes of americium and curium, UCRL-1796, University of California, Radiation Laboratory, 1952

30. Rasumussen JO : Alpha-decay ; Alpha-, Beta-, and Gamma-ray Spectrometry, North-Holland, Amsterdam, 701, 1966

31. Asai M, Tsukada K, Sakama M, Ichikawa S, Ishii T, Nagame Y, Nishinaka I, Akiyama K, Osa A, Oura Y, Sueki K, Shibata M : Experimental identification of spin-parities and single-particle configurations in ^{257}No and its α-decay daughter ^{253}Fm. Phys Rev Lett 95 : 102502, 2005

32. Asai M, Tsukada K, Sakama M, Haba H, Ichikawa S, Ishii T, Nishinaka I, Nagame Y, Kasamatsu Y, Shibata M, Kojima Y, Hayashi H : Ground-state configuration of the N=157 nucleus ^{259}No. Phys Rev C 87 : 014332, 2013

33. Asai M, Sakama M, Tsukada K, Ichikawa S, Haba H, Nishinaka I, Nagame Y, Goto S, Kojima Y, Oura Y, Nakahara H, Shibata M, Kawade K : Proton-neutron configurations in ^{236g,m}Am and its EC-decay daughter ^{236}Pu. Eur Phys J A 23 : 395-400, 2005

34. Sakama M, Tsukada K, Asai M, Ichikawa S, Haba H, Goto S, Nishinaka I, Nagame Y, Oura Y, Kojima Y, Osa A, Shibata M, Kawade K, Ebihara M, Nakahara H : Nuclear decay properties of the neutron-deficient actinides. J Nucl Sci Technol Sup 3 : 34-37, 2002

35. Blann M, Vonach HK : Grobal test of modified precompound decay models. Phys Rev C 11 : 1475-1492, 1983

36. Borschevsky A, Eliav E, Vilkas MJ, Ishikawa Y, Kaldor U : Transition energies of atomic lawrencium. Eur Phys J D 45 : 115-119, 2007